ANTIOXIDANTS & REDOX SIGNALING
Volume 14, Number 12, 2011

DOI: 10.1089/ars.2010.3681

ORIGINAL RESEARCH COMMUNICATION

Astrocytic Redox Remodeling by Amyloid Beta Peptide

Sanjay K. Garg,[1] Victor Vitvitsky,[1] Roger Albin,[2,3] and Ruma Banerjee[1]

Abstract

Astrocytes are critical for neuronal redox homeostasis providing them with cysteine needed for glutathione synthesis. In this study, we demonstrate that the astrocytic redox response signature provoked by amyloid beta (Aβ) is distinct from that of a general oxidant (tertiary-butylhydroperoxide [t-BuOOH]). Acute Aβ treatment increased cystathionine β-synthase (CBS) levels and enhanced transsulfuration flux in contrast to repeated Aβ exposure, which decreased CBS and catalase protein levels. Although t-BuOOH also increased transsulfuration flux, CBS levels were unaffected. The net effect of Aβ treatment was an oxidative shift in the intracellular glutathione/glutathione disulfide redox potential in contrast to a reductive shift in response to peroxide. In the extracellular compartment, Aβ, but not t-BuOOH, enhanced cystine uptake and cysteine accumulation, and resulted in remodeling of the extracellular cysteine/cystine redox potential in the reductive direction. The redox changes elicited by Aβ but not peroxide were associated with enhanced DNA synthesis. CBS activity and protein levels tended to be lower in cerebellum from patients with Alzheimer's disease than in age-matched controls. Our study suggests that the alterations in astrocytic redox status could compromise the neuroprotective potential of astrocytes and may be a potential new target for therapeutic intervention in Alzheimer's disease. *Antioxid. Redox Signal.* 14, 2385–2397.

Introduction

Alzheimer's disease (AD) is a neurodegenerative disorder characterized by extracellular deposition of amyloid beta (Aβ) in senile plaques and intracellular formation of neurofibrillary tangles leading to synaptic loss, neuronal death, and progressive cognitive decline (32). Aβ is a 40–42-amino acid-long peptide derived from amyloid precursor protein. The hydrophobic sequence extending from residues 25–35 in the Aβ peptide are responsible for its aggregation and its neurotoxicity (38).

Astrocytes extend between the neuronal and vascular networks and play critical roles in neurotransmitter, amino acid, energy, and volume homeostasis in brain. Astrocytes also support neuronal redox functions by providing cysteine (15), needed for glutathione (GSH) synthesis. Although the neurotoxicity of Aβ is known to be mediated in part by oxidative stress and reduced antioxidant capacity (12), the effects of Aβ on astrocytic redox metabolism are poorly characterized, despite the key role played by these glial cells in neuronal redox homeostasis under normoxic (8, 14) and stress conditions (15). Aβ activates astroglial cells, stimulating reactive oxygen species (ROS) production, which in turn causes hyperoxidation of plasma membrane proteins and lipids, impaired glutamate clearance with consequent excitotoxicity, and disruption of the mitochondrial membrane potential (3, 12).

Cysteine limits synthesis of GSH, a major intracellular antioxidant. Cysteine can be synthesized *via* the transsulfuration pathway, imported into cells by a specific transporter, ASC, or derived from cystine imported by the x_c- transporter (Fig. 1a). Cystathionine β-synthase (CBS) catalyzes the rate-limiting step in the transsulfuration pathway (9). Faced with oxidative stress conditions depleting the GSH pool, astrocytes mount an autocorrective response by activating the transsulfuration pathway and GSH biosynthesis (Fig. 1b) (47). Mature neurons lack an efficient system for cystine uptake and rely instead on astrocytes for provision of cysteine, which is produced from secreted GSH (Fig. 1a) (14). GSH metabolism is critically interlinked to glutamate-based neurotransmission and ion homeostasis *via* two transporters, x_C- and X_{AG}-, and the Na^+/K^+ ATPase (Fig. 1a). Aberrations at this metabolic nexus are associated with AD (26, 29). Using indirect methods for assessing GSH, two laboratories have reported the effect of Aβ 25–35 on intracellular GSH. However, their results are contradictory. Abramov *et al.* (2) used monochlorobimane to image GSH and reported an $\sim$50% decrease in intracellular GSH levels after 24 h of Aβ treatment. In contrast, Allaman *et al.* (5), using the dithionitrobenzoic acid assay, reported an

Departments of [1]Biochemistry and [2]Neurology, University of Michigan Medical School, Ann Arbor, Michigan.
[3]VAAAHS GRECC, Ann Arbor, Michigan.

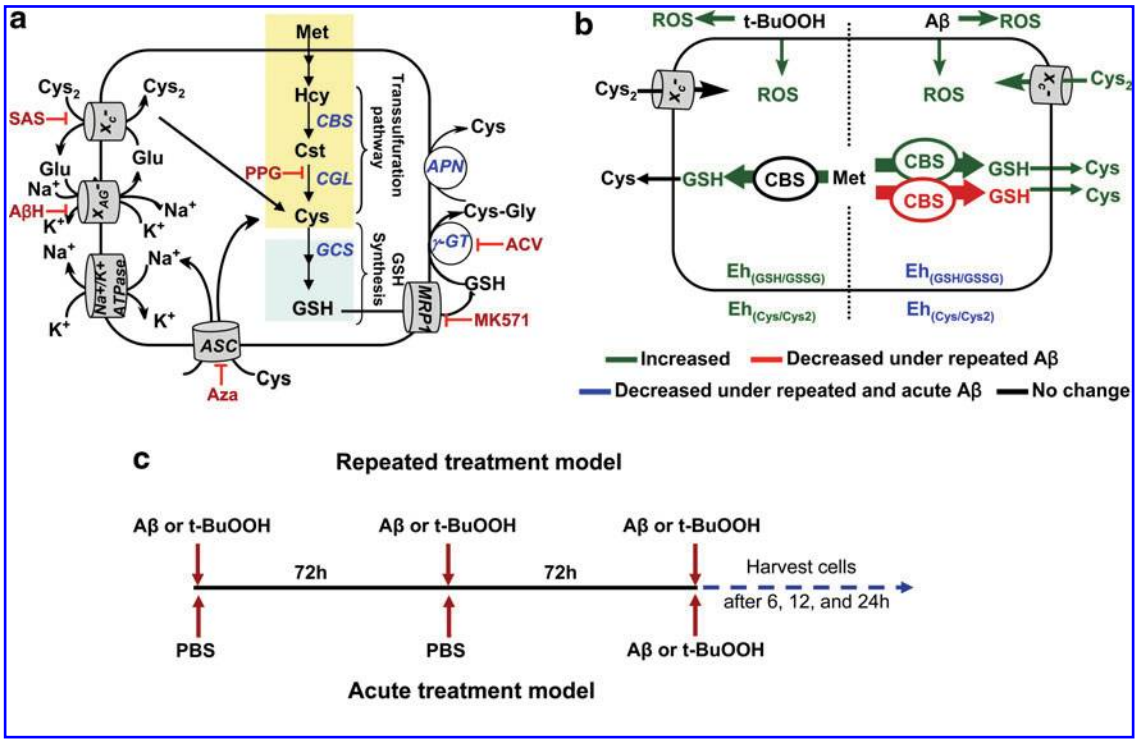

FIG. 1. The effects of specific *versus* general oxidants on the astrocytic thiol-based redox metabolism. (a) Pathway for thiol-based redox metabolism. PPG, SAS, AβH, Aza, ACV, and MK-571 are inhibitors of γ-cystathionase, γ-glutamylcysteinyl synthetase, the x_C- transporter, the X_{AG}- transporter, ASC neutral amino acid transporter, γ-glutamyl transpeptidase (γGT), and the multidrug resistance protein 1 (MRP1), respectively. **(b)** Differences in the redox responses elicited by Aβ *versus* t-BuOOH. *Green lines* and *fonts* denote metabolites or activities that increase in response to acute or repeated treatment conditions; *blue* denotes a decrease under acute and repeated Aβ but not t-BuOOH treatment conditions, and *red* denotes a decrease only with repeated Aβ treatment. *Black lines* and *text* represent denote parameters in which no changes were observed. **(c)** Scheme showing the treatment regimens for acute *versus* repeated exposure to Aβ or t-BuOOH. Aβ, amyloid beta; AβH, aspartate-β-hydroxamate; ACV, acivicin; Aza, azaserine; PPG, propargylglycine; t-BuOOH, tertiary-butylhydroperoxide; SAS, sulfasalazine.

~300% increase in extracellular GSH with no change in intracellular GSH levels after 48 h of Aβ treatment. The mechanism of GSH extrusion and modulation of its concentration by Aβ were not investigated.

In this study, we have examined the effects of acute and repeated Aβ treatment on astrocytic GSH biosynthesis, redox potential, and the transsulfuration pathway and compared them with the effects elicited by tertiary-butylhydroperoxide (t-BuOOH) treatment. We find that both short and repeated Aβ treatment induce a reductive redox potential in the extracellular milieu but an oxidative shift in the intracellular compartment. Acute Aβ treatment increased CBS levels and enhanced transsulfuration flux in contrast to repeated Aβ exposure, which decreased CBS and catalase protein levels. Further, Aβ orchestrates an intracellular response, which is mechanistically distinct from that of a nonspecific oxidant, including changes in CBS and catalase protein levels and DNA synthesis that are not seen with t-BuOOH treatment. CBS levels and activity appear to be lower in the cerebellum of AD brains than in age-matched controls, indicating a pathological relevance for the *ex vivo* observation. These results reveal the importance of identifying disease-specific redox signatures, which could have the potential for development of metabolism-based disease-modifying therapeutic approaches.

Materials and Methods

Biological samples

AD brain and age-matched control samples were from the Michigan Alzheimer's Disease Research Center Brain Bank. AD samples were derived from clinically well-characterized individuals participating in a prospective brain collection program. At death, one hemisphere was cut into 1–1.5 cm coronal slabs and frozen rapidly over liquid N_2 vapor and stored in heat-sealed freezer bags at −80°C until use. The other hemisphere was fixed in 10% neutral buffered formalin and used for neuropathologic analysis. All specimens are reviewed by the same neuropathologist and diagnosis established by the Reagan-NIA criteria (13). Age, gender, and postmortem delay-matched control specimens were derived from individuals with no clinical history of neurologic disease and normal neuropathologic examinations. Slabs were warmed to −20°C and blocs of frontal cortex and cerebellum were prepared. The University of Michigan's Committee on Use and Care of Animals approved the protocol used in this study for handling animals.

Isolation and preparation of murine primary cells

Primary murine cortical astrocytes cultures were prepared from 1- to 2-day-old Balb/c pups as described previously (20,

21). At the end of the third passage, cells were seeded in 6-well (2×10^6 cells/well/2 ml), 24-well (5×10^5 cells/well/ml), or 48-well plates (5×10^4 cells/well/0.4 ml), or a 8-well chamber slide (1×10^5 cells/well/0.4 ml), depending on the experiment, and incubated for a week (with half the medium being changed every third day). The purity of astrocytes was determined as described previously (21) and was $\geq$93%.

Dissociated neurons were prepared as described previously from embryonic day 16 (E16) to E18 mice and cultured (1×10^5 cells/well/0.5 ml) in neurobasal media containing B27 (1×) supplement, 2 m*M* L-glutamine and penicillin–streptomycin (100 units/ml and 100 μg/ml final concentration, respectively) on laminin (Invitrogen) and poly-D-lysine (Sigma)-coated glass cover slips (12 mm; Bellco Glass) in 24-well plates (20, 21). The purity of neurons was assessed by staining with antibody to anti-β III tubulin (TUJ1) and found to be >95% as observed microscopically.

Aggregation of Aβ peptide

The lyophilized form of the triflouroacetate salt of the Aβ peptide (25–35, or 1–42 Bachem) was aggregated as described previously (37). Briefly, Aβ was dissolved in sterile double-distilled water as a 2 m*M* stock solution, incubated for 8 days at 37°C, and stored in aliquots at −80°C. Soluble Aβ (2 m*M*) was prepared by dissolving lyophilized peptide in 1% dimethyl sulfoxide and stored immediately at −80°C.

Aβ treatment of primary astrocyte cultures

At the start of experiments, astrocytes were replenished with fresh astrocyte media (Dulbecco's modified Eagle's medium/F12 + 2 m*M* L-glutamine + 10% heat inactivated fetal bovine serum + penicillin-streptomycin (100 units/ml and 100 μg/ml final concentration, respectively). For the acute treatment, a single bolus of 200 μ*M* t-BuOOH or 50 μ*M* Aβ (25–35) or 10 μ*M* Aβ (1–42) was added and incubation was continued for the desired times (Fig. 1c). For the repeated treatment model, astrocytes were stimulated with 50 μ*M* Aβ (25–35) or 10 μ*M* Aβ (1–42) repeatedly (3 bolus treatments, once every 72 h), and experimental analysis was started after the third Aβ treatment (Fig. 1c). Cell death was observed in <10% of astrocytes after acute or repeated Aβ treatment as monitored by the PI-AV labeling kit (data not shown; BioVision) and TUNEL assay kit (Roche) according to the vendor's protocol. Sulfasalazine (SAS, 500 μ*M*), MK571 (100 μ*M*), acivicin (400 μ*M*), azaserine (500 μ*M*), and aspartate-β-hydroxamate (400 μ*M*) (Sigma) when used were added in a single bolus at the start of the acute Aβ treatment or the third exposure to repeated Aβ treatment regimen. The effect of Aβ dose on astrocyte viability and metabolite levels was determined after a single bolus treatment with 1, 10, or 50 μM Aβ (acute model) or with the same Aβ concentrations but administered using the repeated treatment regimen described above. To study the response of the transsulfuration pathway during acute and repeated stimulation with either t-BuOOH or Aβ, cells were incubated with L-(^{35}S)-methionine (Perkin Elmer) to a final concentration of 2 μCi/ml in the presence or absence of 2.5 m*M* propargylglycine for 6 or 12 h. At the indicated time points, culture supernatants were removed and used immediately for H_2O_2 analysis or stored frozen at −80°C until used for determination of extracellular thiols. Cells were harvested and frozen at −80°C until further use.

CBS analysis in the human brain samples

Frozen brain tissue (~300 mg) was pulverized in liquid N_2 and CBS activity and protein expression in the postmortem brain samples of patients with AD and age-related normal subjects were analyzed as described previously (46).

Metabolite analyses

Extracellular thiols (cystine, cysteine, and GSH) in cell culture medium were quantified in metaphosphoric acid-fixed protein-free supernatant as described previously (20, 35). Intracellular GSH and incorporation of (^{35}S) from methionine into GSH was quantified as described previously (20, 35). The results were normalized to the protein concentration in each sample.

(^{3}H)-thymidine incorporation assay

Astrocytes (5×10^4/well) were seeded at ~50%–70% confluency in 48-well plates at day 0. After stimulation with Aβ (25–35) or t-BuOOH for 2 h, cells were incubated with (^{3}H)-thymidine (1 μCi/ml; Perkin Elmer) for a further ~24 h at 37°C. Cells were washed twice with phosphate-buffered saline (PBS) and dissolved in 100 μl NaOH (0.2 M). The samples were mixed with scintillation cocktail and radioactivity incorporation was measured.

Western blot analysis

Astrocytes with the indicated treatments and at the desired time points were harvested and lysed on ice as described previously (19). Antibodies against CBS, catalase, superoxide dismutase 1 (SOD1) (Abcam), actin (Sigma), and xCT, the catalytic subunit of x_C- (Novus Biological), were used to monitor expression of the respective protein antigens and detected using the Dura chemiluminescent horseradish peroxidase system (Pierce).

Determination of extracellular H_2O_2 and intracellular ROS

Astrocytes were treated with a single bolus of the 25–35 Aβ peptide for 3 and 24 h acutely or repeatedly as described above. To check the effect of antioxidant on ROS production, astrocytes were pre-treated or not with 1 m*M* N-acetyl cysteine (NAC) for 24 h and then incubated with Aβ 25–35 (50 μ*M*) or 1–42 (10 μ*M*) for 3 h. Alternatively, astrocytes were transfected with catalase-His-V5-expressing pCDNA3.1 (a generous gift from Brent Carter, University of Iowa) or the empty pCDNA3.1 plasmid using TransIT-2020 reagent (Mirus) as per the manufacturer's protocol. After 24 h post transfection, cells were incubated with Aβ 25–35 (50 μ*M*) or 1–42 (10 μ*M*) in fresh media for 3 h. After Aβ stimulation, the astrocyte conditioned medium was saved for extracellular H_2O_2 determination, whereas the cells were used for intracellular ROS detection using the Image-iT Live Green ROS Detection Kit as per the manufacturer's protocol (Invitrogen). Briefly, cells were washed twice with Ca^{2+}- and Mg^{2+}-free Hank's balanced salt solution (HBSS), followed by incubation with 5-(and-6)-carboxy-2′,7′-dichlorodihydrofluorescein diacetate (Invitrogen) at a final concentration of 5 μ*M* for 30 min at 37°C. Cells were washed once with HBSS and incubated with Hoechst 33342 nuclei stain (1:200 dilution, excitation 365 nm, emission 480 nm; Invitrogen) for 10 min at 37°C to ensure equal cell numbers. Cells were washed three times with HBSS followed by lysing using the lysis buffer. An aliquot of lysate

(100 μl each) was transferred to a fluorimetric plate, the fluorescence excitation/emission maxima were recorded at 495/529 nm and the results expressed as F529/F480 nm. The concentration of H_2O_2 in the conditioned media was measured using the Amplex Red reagent kit as per the manufacturer's protocol (Molecular Probe). Conditioned media (100 μl) in a 96-well fluorimetric plate was mixed with 10 μM Amplex red reagent and 1 U/ml horseradish peroxidase at a 1:1 ratio and incubated for 30 min at room temperature. A standard curve was generated with known concentrations (50 nM to 10 μM) of H_2O_2. The amount of resorufin produced by Amplex Red oxidation was determined fluorimetrically (excitation: 544 nm, emission: 590 nm). Background fluorescence was determined for the medium control and subtracted from each value and results were expressed as the concentration of H_2O_2 in the medium.

Analysis of apoptosis

The terminal deoxynucleotidyl transferase-dUTP nick end labeling (TUNEL) assay (Roche Diagnostics) was employed as previously described (20). Briefly, astrocytes were cultured in 24-well plates and treated acutely or repeatedly with 50 μM (25–35) or 10 μM (1–42) Aβ as described above. After incubation, 500 μl of each conditioned media was transferred on to neuronal monolayers in 250 μl neuronal media in the presence or absence of 50 μM Aβ (25–35). Neurons were incubated for another 12–14 h followed by labeling with the TUNEL stain. To check the effect of Aβ or t-BuOOH on viability, astrocytes were treated with different concentrations of Aβ (25–35) peptide (1, 10, 50 μM) or t-BuOOH (200, 400, 800 μM) for 12–14 h followed by labeling with the TUNEL stain. Nuclei were observed with Hoechst stain (1:200 dilution, excitation 365 nm, emission 480 nm; Invitrogen) and quantitative analysis was performed by counting >2000 cells as described previously (20).

Analysis of mitochondrial activity

To check the effect of Aβ on astrocytic mitochondrial activity, the 3-(4,5-dimethylthiazol-2yl)-2,5-diphenyltetrazolium bromide (MTT) assay was employed as previously described (47). In brief, astrocytes (1×10^6/well) in 24-well plates were treated with different concentration of Aβ (25–35) acutely or repeatedly. After stimulation for ~20 h, cells were washed with PBS and incubated with MTT dye (0.5 mg/ml) for 2 h at 37°C, followed by washing with PBS. Cells were dissolved in dimethyl sulfoxide. Optical density was measured at 553 nm and the background was corrected after reading the absorbance at 650 nm.

Statistical analyses

The significance of the differences in data between control and experimental groups was determined by one-way analysis of variance followed by post-test Bonferroni adjustment. Students *t*-test (paired, two-tailed) was also performed for comparison with the analysis of variance test. $p<0.05$ was considered to be statistically significant.

Results

Protracted increase in astrocytic ROS production by Aβ

Since the kinetics of Aβ-induced ROS production by astrocytes and microglia have previously been monitored only on a short time scale (3, 24), we examined the intracellular ROS and extracellular H_2O_2 levels on a longer time scale during which metabolic changes are typically observed (Fig. 2). Acute Aβ treatment was reported to induce an ~2-fold increase in ROS levels 30 min after exposure (3). We found similarly increased ROS levels even at 3 h after acute Aβ (25–35) exposure, but the levels declined to control values after 24 h (Fig. 2a). In contrast, intracellular ROS levels were ~3- and ~5-fold higher at the same times after the last Aβ (25–35) addition in the repeated treatment regimen (Fig. 2a). Since ROS are typically short-lived, these results reveal that both acute and repeated Aβ-treatment regimens provoke sustained ROS production spanning several hours. ROS production is paralleled by increased extracellular H_2O_2, with the kinetics of H_2O_2 increase and dissipation varying with the treatment regimen. Extracellular H_2O_2 levels were ~4-fold higher after 24 h of acute and ~2-fold higher after 24 h of repeated Aβ treatment (Fig. 2b). The longer Aβ (1–42) peptide increased intracellular ROS by ~50% and extracellular H_2O_2 by ~65% after 3 h of treatment (Fig. 2c, d). Addition of the antioxidant, NAC, a cysteine precursor, or over expression of catalase, a peroxide scavenger, decreased Aβ-mediated over production of ROS (Fig. 2c, e) and H_2O_2 (Fig. 2d, f). When freshly prepared 50 μM Aβ (25–35) was used instead of the aggregated form, it failed to induce over production of intracellular ROS and extracellular H_2O_2 (Fig. 2g, h). Catalase, SOD, and GSH peroxidase are major antioxidant enzymes in mammalian cells that clear ROS. We checked the expression levels of two of these antioxidant enzymes and found that repeated but not acute Aβ (25–35) treatment decreased steady-state levels of catalase, whereas Cu/Zn SOD1 was unchanged by either treatment (Fig. 2i). In contrast, neither acute nor chronic t-BuOOH treatment affected catalase or SOD1 expression levels (Fig. 2i). Since the magnitude of ROS stimulation seen with Aβ (25–35) and (1–42) was similar, and NAC similarly abrogated ROS accumulation, further experiments were conducted with the shorter peptide.

Differential responses in transsulfuration and GSH synthesis pathways to acute versus repeated Aβ *treatment*

One mechanism by which human astrocytes respond to oxidative stress induced by t-BuOOH is by increasing flux through the transsulfuration pathway (47), which furnishes cysteine and results in increased GSH synthesis. In murine astrocytes, acute t-BuOOH or acute Aβ (25–35) stimulation also induced GSH synthesis at levels that were comparable at 6 and 12 h (Fig. 3a). When freshly prepared 50 μM soluble Aβ (25–35) was used, no change in GSH levels was observed at 6 h (Fig. 3b). An ~50% increase in radiolabel incorporation from (^{35}S)-methionine to GSH was observed in 6 h upon acute t-BuOOH or acute Aβ stimulation (Fig. 3c) that was inhibited ~2-fold by propargylglycine, a suicide inhibitor of γ-cystathionase, the second enzyme in the transsulfuration pathway (Fig. 1a), demonstrating the role of this pathway in the astrocytic response to acute oxidative challenge. In contrast, GSH levels were unchanged by repeated treatment with either t-BuOOH or Aβ (25–35) after 6 h and diminished ~20% with Aβ after 12 h (Fig. 3a). Repeated Aβ treatment (25–35) resulted in an ~2-fold decrease in the transsulfuration flux (Fig. 3d). Glutathione disulfide (GSSG) levels were ~3-fold higher in response to t-BuOOH at 6 h but normalized to control levels at 12 h (Fig. 3e). In contrast, acute Aβ

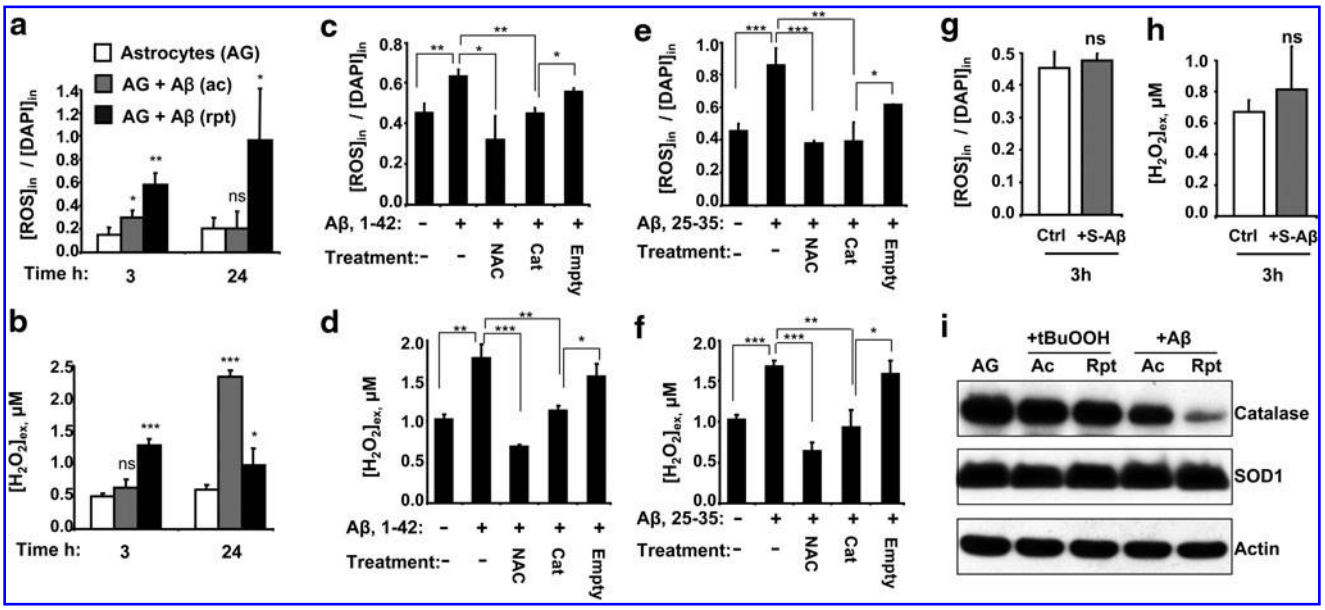

FIG. 2. Antioxidant (NAC or catalase) treatment abrogates Aβ-mediated ROS generation in astrocytes. (a, b) Astrocytes (AG) were incubated with none (*white bar*), 50 μ*M* Aβ 25–35 acute (*gray bar*), or repeated (*black bar*), and intracellular ROS levels **(a)** and extracellular H_2O_2 **(b)** were measured either 3 or 24 h later. Astrocytes were either treated with 1 m*M* NAC or transfected with a catalase expression or empty vector for 24 h and then treated with either 10 μ*M* Aβ 1–42 **(c, d)** or 50 μ*M* Aβ 25–35 **(e, f)** for 3 h and intracellular ROS **(c, e)** and extracellular H_2O_2 **(d, f)** were measured. **(g, h)** Freshly prepared soluble Aβ (*gray bar*, S-Aβ, 25–35) does not provoke ROS (g) and H_2O_2 (h) production in astrocytes, respectively. **(i)** The effect of Aβ (25–35) *versus* t-BuOOH treatment on astrocytic catalase and SOD1 expression. Data are the mean ± SD representative of two independent experiments each performed in triplicate. $^*p \le 0.05$, $^{**}p \le 0.01$, $^{***}p \le 0.001$; ns, not significant. NAC, N-acetyl cysteine; ROS, reactive oxygen species; SOD, superoxide dismutase.

treatment (25–35) caused a slower increase in GSSG levels, which were 20% higher at 6 h and twofold higher at 12 h in comparison to the untreated control. An effect on the GSSG concentration was not observed with repeated t-BuOOH and Aβ treatment. As a result of the varied responses in the GSH and GSSG pool with different treatments, the GSH:GSSG ratio, an indicator of the intracellular redox poise, initially decreased in response to acute (~30%) and repeated (~50%) t-BuOOH treatment at 6 h but subsequently overshot control values at 12 h (Fig. 3f). In contrast, both acute and repeated Aβ treatments resulted in an oxidative shift in the intracellular GSH/GSSG ratio.

CBS catalyzes the committing step in the transsulfuration pathway and Western blot analysis revealed that CBS protein levels increase in response to acute treatment with Aβ (25–35) but decrease in response to repeated treatment (Fig. 3g). In contrast, neither acute nor repeated t-BuOOH affected CBS levels. Hence, the astrocytic redox responses to Aβ *versus* an organic peroxide challenge and to acute- *versus* repeated exposure to Aβ are distinct.

Aβ induces oxidative remodeling of the intracellular GSH/GSSG redox potential

The GSH/GSSG potential is initially slightly oxidized at 6 h in response to acute (−241 mV) and repeated (−244 mV) t-BuOOH treatment compared with control (−247 mV) but subsequently overshoots the control value by appoximately −10 mV at 12 h (Fig. 3h). In contrast, acute Aβ treatment (25–35) results in an oxidative shift in the GSH/GSSG potential to −237 mV at 12 h, whereas repeated Aβ treatment elicits the same change within 6 h.

Aβ induces reductive remodeling of the extracellular cysteine/cystine redox potential

The cysteine:cystine ratio is a key determinant of the extracellular redox poise (33). Hence, the kinetics of extracellular cystine consumption and cysteine accumulation were monitored and were strikingly more rapid in the presence of Aβ (25–35) than in untreated controls (Fig. 4a, b) and dependent on the dose of Aβ (Fig. 5a, b). Aβ (1–42) caused similar changes in cysteine and cystine (data not shown). Levels of xCT, the catalytic subunit of the primary cystine transporter, x_C^-, were not affected by acute Aβ (25–35) treatment but were downregulated >4-fold with repeated Aβ treatment (Fig. 4c). Neither acute nor repeated t-BuOOH treatment influenced xCT levels (Fig. 4c) or affected cystine consumption significantly (data not shown). The cysteine/cystine redox couple is important for controlling the redox poise in the extracellular space. The extracellular cysteine/cystine redox potential in untreated cells was estimated to be appoximately −80 mV at 2 h. After 6 h of culture, the redox potential decreased to −90 mV (untreated controls) *versus* −105 mV (acute Aβ treatment) and −124 mV (repeated Aβ treatment), indicating a more reducing environment (Fig. 4d) and the magnitude of the reductive shift was dependent on the dose of Aβ (Fig. 5c). As expected, t-BuOOH caused cysteine oxidation and the redox potential increased to a more positive value at 2 h but normalized to control values in 6 h (Fig. 4d). Neither acute nor repeated t-BuOOH treatment altered the extracellular GSH concentration, whereas a time-dependent increase in extracellular GSH was observed in response to Aβ treatment (Fig. 4e), which was dependent on the dose of Aβ (Fig. 5d). Thus,

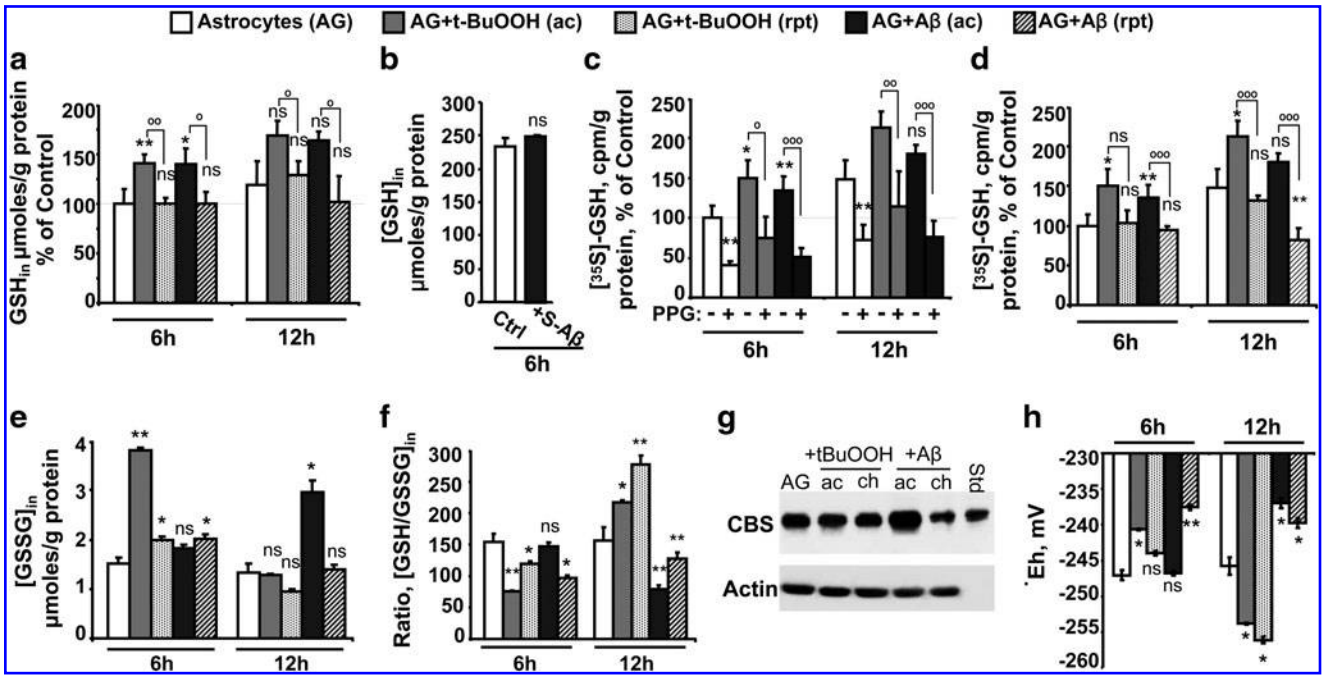

FIG. 3. Astrocytes upregulate the transsulfuration pathway during acute treatment with t-BuOOH or A*β*. Astrocytes (AG) were treated with either none (*white bar*) or acutely with a single bolus of either 200 μM t-BuOOH (*gray bar*) or 50 μM Aβ (25–35, *black bar*) and incubated together with (^{35}S)-methionine ± 2.5 m*M* PPG for 6 and 12 h. To compare the GSH level under acute and repeated treatment, astrocytes were either untreated or treated acutely or repeatedly with 200 μM t-BuOOH or 50 μM Aβ (25–35). At the indicated times, cells were harvested and intracellular (GSH) **(a),** (GSSG) **(e)** and radioactivity incorporation in GSH **(c, d),** were measured, normalized to protein level and ratio of GSH/GSSG was calculated **(f)**. Intracellular (GSH) in untreated astrocytes was 298 ± 87 pmol/μg protein and 354 ± 141 μmol/g protein at 6 and 12 h, respectively. The radioactive counts in GSH were 691 ± 94 cpm/μg protein and 1096 ± 284 cpm/μg protein at 6 h and 12 h post-incubation with (^{35}S)-methionine. **(b)** shows the effect of freshly dissolved soluble 50 μM Aβ (*black bar*, S-Aβ, 25–35) on astrocytic GSH. The Western blot data in **(g)** shows CBS in astrocytes after acute or repeated treatment with either t-BuOOH or Aβ (25–35) for 24 h. **(h)** shows the intracellular GSH/GSSG redox potential that was calculated using the Nernst equation: $E_h = E_o + RT/nF \ln([GSSG]/[GSH]^2)$, using $E_o = -240$ mV (pH = 7.4). Data are represented as % mean ± SD of 5 **(a, c, d, h)** or 2 **(b, g)** or three independent experiments **(e, f),** each performed at least in duplicate on different batches of cells. *,°$p \le 0.05$; **,°°$p \le 0.01$; °°°$p \le 0.001$; ns, not significant. Asterisks (*) denote the level of significance in the comparison between untreated *versus* treated conditions, whereas the open circles (°) represent the comparison between acute and repeated treatments with the same agent. GSH, glutathione; CBS, cystathionine β-synthase; GSSG, glutathione disulfide.

the metabolic response both inside and outside the cell to Aβ-induced increase in ROS levels results in reductive remodeling in the extracellular compartment.

Aβ induces DNA synthesis

Since a reductive shift in the extracellular potential is usually correlated with cell proliferation, the effect of Aβ (25–35) on DNA synthesis was assessed. Like dendritic cells that remodel the extracellular redox potential to support T cell proliferation (49), the astrocytic response to Aβ might similarly stimulate a proliferative glial response. Acute Aβ treatment increased (^{3}H)-thymidine incorporation into DNA by ~50% (Fig. 6) as seen previously (27), while a robust 300% increase was observed with repeated Aβ treatment. In contrast, t-BuOOH decreased (^{3}H)-thymidine incorporation into DNA modestly when applied as a single bolus, whereas repeated t-BuOOH treatment resulted in a 200% decrease (Fig. 6).

Intracellular GSH is source of extracellular cysteine

Extracellular cysteine is derived from the breakdown of secreted GSH *via* the γ-glutamyl pathway (49). To establish the involvement of this pathway in the astrocytic response to Aβ (25–35), we employed pharmacological inhibition at various steps (Fig. 1a). Inhibition of cystine import with SAS, GSH export with MK-571, or extracellular GSH cleavage with acivicin significantly decreased extracellular cysteine accumulation (Fig. 7a). In contrast, inhibition of X_{AG}^-, which has a low affinity for cysteine, or inhibition of ASC, the neutral amino acid transporter, did not have a significant effect on extracellular cysteine accumulation. Of these inhibitors, only SAS and to a smaller extent, MK-571, diminished cystine consumption from the medium (Fig. 7b). whereas the decrease in cystine consumption in the presence of SAS is expected, the effect of MK-571 might be indirect, that is, by inhibiting GSH efflux, it inhibits cystine uptake.

Aβ does not cause astrocytic apoptosis but decreases mitochondrial activity

Aβ-mediated cellular toxicity and apoptosis are reported in AD (3, 5, 6) and primary neurons are very sensitive to Aβ-induced apoptosis. Astrocytes exposed to 50 μM Aβ (25–25)

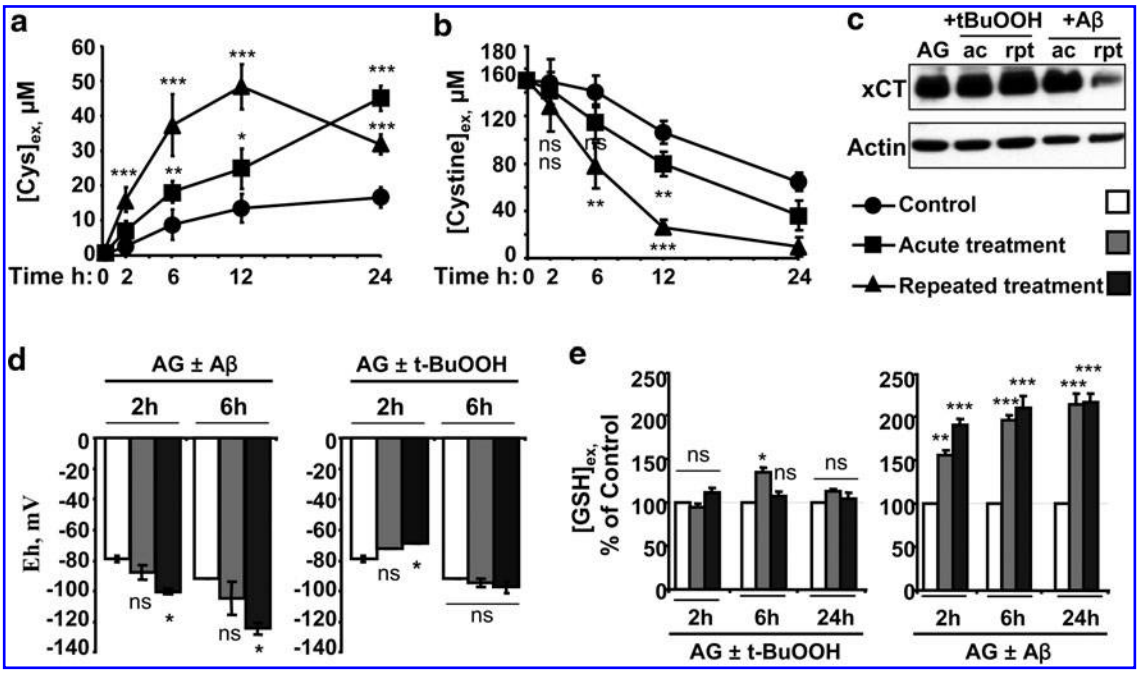

FIG. 4. Changes in the extracellular cysteine/cystine redox potential in response to t-BuOOH or Aβ treatment. Astrocytes were either untreated (*circle* or *while bar*) or treated acutely (*square* or *gray bar*) or repeatedly (*triangle* or *balck bar*) with 50 μM Aβ (25–35) or 200 μM t-BuOOH. Extracellular cysteine **(a)**, cystine **(b)**, and GSH **(e)** concentrations were determined in aliquots removed from the culture medium. In **(a)**, the concentration of cysteine in the medium at time 0 (15 ± 5.7 *μM*) was subtracted from the values at all time points. **(c)** shows the effect of Aβ *versus* t-BuOOH treatment on astrocytic xCT expression. **(d)** The extracellular cysteine/cystine redox potential when astrocytes were treated with 200 *μM* t-BuOOH or 50 *μM* Aβ was calculated using the Nernst equation (Fig. 3 legend), using $E_o = -250$ mV (pH = 7.4). Data are the mean ± SD of 4 **(a, b, d, e)** or 2 **(c)** independent experiments performed on different batches of cells. Asterisks ($*p \le 0.05$, $**p \le 0.01$, $***p \le 0.001$) denote the level of significance in the comparison between untreated and treated conditions. ns, not significant.

are resistant to apoptosis after exposure to Aβ (25–35) as monitored by the TUNEL (Fig. 8a) or Annexin-V (data not shown) assays. In contrast, 800 *μM* t-BuOOH induced apoptosis in ~80% of the astrocytes but not at 400 μM (not shown) as measured using the TUNEL assay. Interestingly, the MTT assay, a reporter of mitochondrial activity, showed a dose-dependent decrease (~10%–35%) in response to Aβ (25–35) treatment, which was concentration dependent (Fig. 8b). In contrast, 200 μM t-BuOOH did not show a significant reduction of MTT (data not shown).

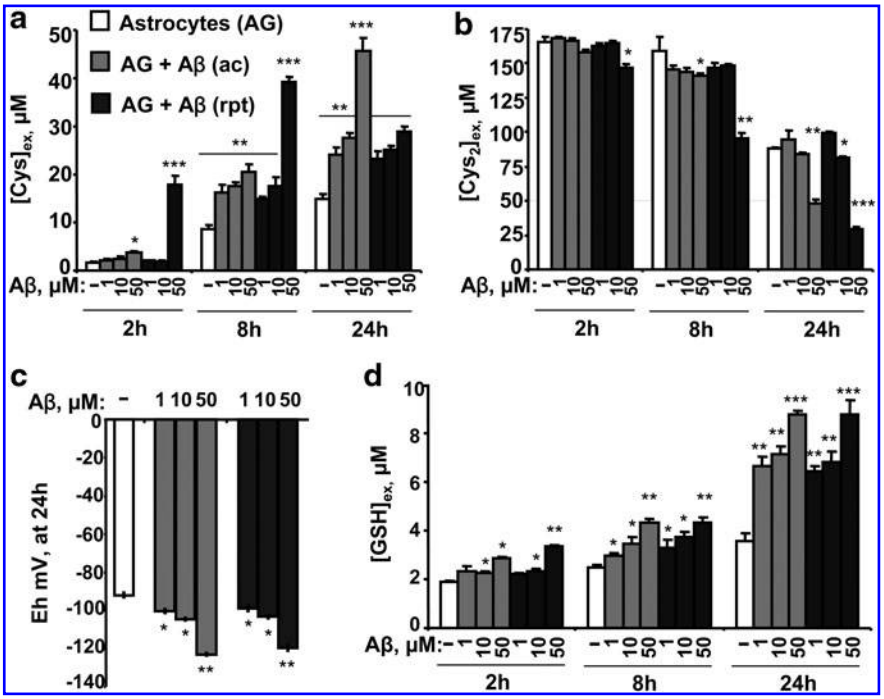

FIG. 5. Dose dependence of Aβ on the extracellular cysteine/cystine redox couple. Astrocytes were either untreated (*white bar*), or treated acutely (*gray bar*) or repeatedly (*black bar*) with 1, 10, and 50 *μM* of Aβ (25–35). At the indicated time, an aliquot of culture supernatant was collected and extracellular cysteine (Cys) **(a)**, cystine (Cys_2) **(b),** and GSH **(d)** were measured, and the redox potential **(c)** was calculated as described in Fig. 4 legend. Data are mean ± SD from two independent experiments each performed in triplicate on different batches of cells. Asterisks ($*p \le 0.05$, $**p \le 0.01$, $***p \le 0.001$) denote level of significance and are shown only if there was a statistically significant difference and represent the comparison between untreated controls and treated conditions.

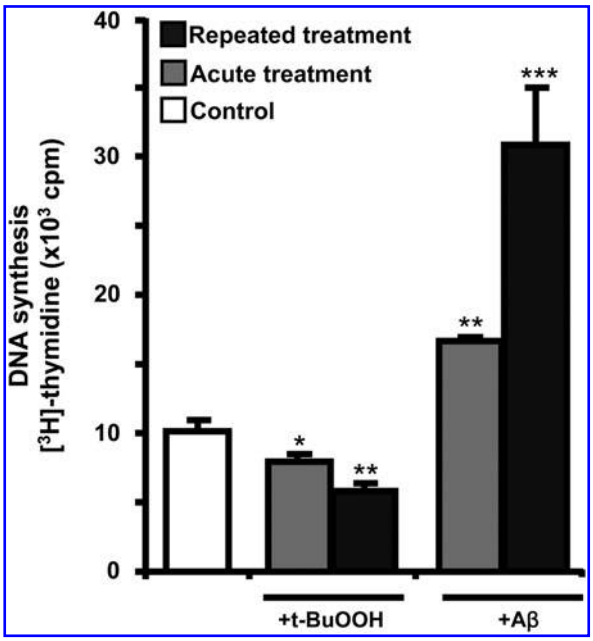

FIG. 6. DNA synthesis is induced by Aβ but not by peroxide. After acute or repeated treatment with Aβ or t-BuOOH, cells were incubated with (^{3}H)-thymidine (1 μCi) for ~24 h at 37°C, before radioactivity incorporation was measured. Data are mean ± SD from two independent experiments each performed in triplicate on different batches of cells. Asterisks (*) represent the level of significance for comparison between untreated and treated samples as indicated in Fig. 5 legend.

Repeated Aβ treatment abrogates the neuroprotective effect of astrocytes

Cysteine enhances GSH synthesis in neurons and is a known neuroprotectant (15). Since Aβ stimulates extracellular cysteine accumulation by astrocytes, the effect of astrocyte-conditioned media on protecting neurons from Aβ-induced apoptosis was examined. For this, astrocytes were stimulated acutely or repeatedly with 50 μM Aβ (25–35) or 10 μM Aβ (25–35) as described under the Materials and Methods section and after 12–14 h of incubation, conditioned medium was removed and transferred onto neuronal monolayers in the presence or absence of 50 μM Aβ for 12–14 h after which apoptosis was assessed by the TUNEL assay (Fig. 9). Unlike astrocytes that were not found to undergo apoptosis in response to 50 μM Aβ treatment (Fig. 8a), ~50% neuronal cell death was observed. Conditioned medium from untreated or acutely treated astrocyte cultures afforded similarly modest but significant protection of neurons from apoptosis compared with fresh medium (Fig. 9a, b). In contrast, when conditioned medium from astrocyte cultures exposed to repeated Aβ treatment was used, the neuroprotective effect was abrogated (Fig. 9a, b). The effect of astrocyte-conditioned medium from cultures that had received either acute or repeated Aβ treatment regimens on survival of neurons that had not been exposed to Aβ was assessed (Fig. 9c). Conditioned media from either untreated or acutely treated astrocytes (with either Aβ 25–35 or 1–42) did not cause neuronal toxicity. However, conditioned media from astrocytes exposed to the repeated Aβ regimen caused significant neuronal apoptosis (Fig. 9c). Notably, the extent of chronic Aβ 1–42-mediated apoptosis was considerably lower than for Aβ 25–35 (Fig. 9c).

Changes in CBS levels and activity in AD brain

Immunohistochemical localization of CBS in adult murine brain reveals weak and diffuse labeling with the exception of the hippocampus and cerebellum, where the labeling is intense (42). Since cerebellar and cortical tissues from AD patients and age-matched controls were more readily available than hippocampal tissue, we compared CBS activity and protein levels in these samples (Fig. 10). Although differences were not observed in the frontal cortex, cerebellum from AD patients tended to exhibit both lower CBS expression (Fig. 10a, b) and activity (Fig. 10c). However, due to high variations and relatively low sample number, the difference did not reach statistical significance. Moreover, differences in CBS protein level and activity between AD and healthy subjects did not correlate with sex, age, and postmortem time of the individual specimens (Supplementary Table S1; Supplementary Data are available online at www.liebertonline.com/ars).

Discussion

While oxidative stress is a nonspecific hallmark of many neurodegenerative diseases (6), the sequelae of specific redox potential changes in the intra- *versus* extra-cellular compartments that govern disease-specific signaling and metabolic responses are unknown. Since H_2O_2 is reported to mediate Aβ

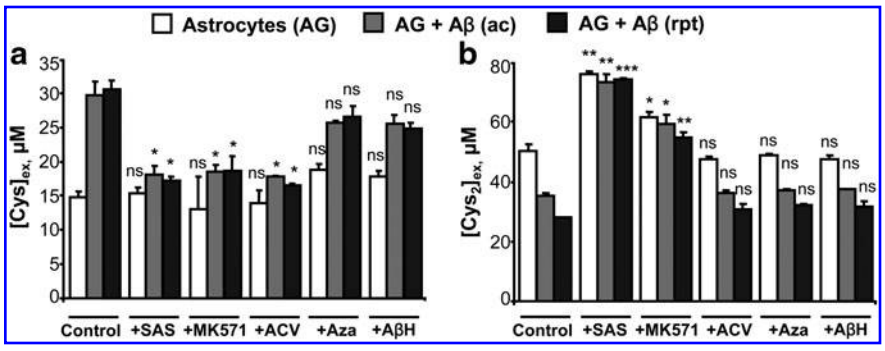

FIG. 7. The γ-glutamyl cycle is a primarily responsible for cysteine release from astrocytes. Astrocytes (AG) were either untreated (*white bar*), or treated acutely (*gray bar*) or repeatedly (*black bar*) with 50 μM Aβ (25–35) ± different inhibitors. At 24 h post-incubation, an aliquot of the culture supernatant was collected and extracellular (Cys) **(a)** and (Cys_2) **(b)** were measured. Data are the mean ± SD from 3 independent experiments each performed in duplicate on different batches of cells. Asterisks ($*p \le 0.05$, $**p \le 0.01$, $***p \le 0.001$) denote statistical significance in extracellular (Cys) between AG control ± inhibitors or AG + Aβ acute ± inhibitors or AG + Aβ repeated ± inhibitors. ns, not significant.

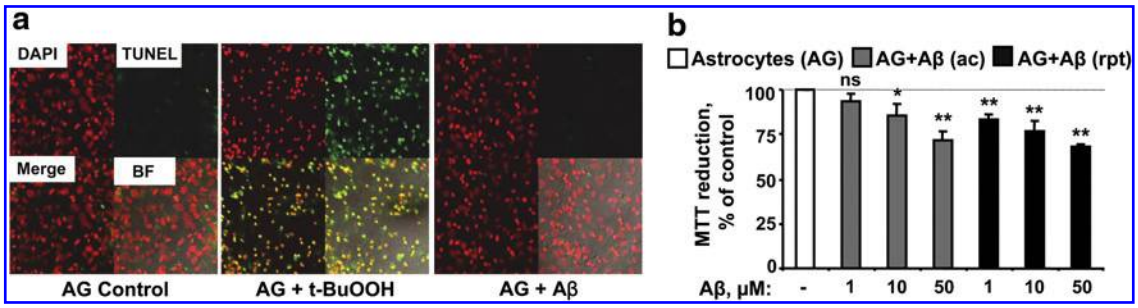

FIG. 8. Aβ does not cause astrocytic cell death but impairs the mitochondrial activity in a dose-dependent manner. (a) After stimulation with Aβ (50 μM; 25–35) or t-BuOOH (800 μM), the extent of astrocytic apoptosis was determined using the TUNEL assay. To permit quantitative analysis, nuclei were stained with Hoechst stain (excitation 365 nm, emission 480 nm). *Red* and *green* colors show staining for nuclei and apoptotic cells respectively. Merge represents the overlap of *red* and *green*; BF denotes bright-field contrast enhancement of the merged image. **(b)** After addition of different concentrations of Aβ (25–35, acute or repeated) stimulation for ~20 h, cells were washed with phosphate-buffered saline, and incubated with MTT dye (0.5 mg/ml) for 2 h at 37°C, followed by washing in phosphate-buffered saline, dissolving in dimethyl sulfoxide, and reading the optical density at 553 nm. **(a)** shows representative data from two independent experiments. **(b)** shows data as mean ± SD from 3 independent experiments each performed in triplicate on different batches of cells. $^{*}p \leq 0.05$, $^{**}p \leq 0.01$, ns = not significant. TUNEL, terminal deoxynucleotidyl transferase-dUTP nick end labeling.

toxicity (11), we investigated thiol-based redox responses of astrocytes to Aβ *versus* the organic peroxide, t-BuOOH, and discovered that they elicit significantly different effects (Fig. 1b).

Cellular functions such as proliferation, differentiation, and death signals are modulated in part by the intracellular and extracellular redox potentials (43). Mammalian cells have multiple redox buffering systems (22). The redox potential of the extracellular compartment is regulated dynamically by intracellular redox metabolism, and, in contrast to the importance of the GSH/GSSG redox couple inside the cell, the cysteine/cystine redox pair is quantitatively the most

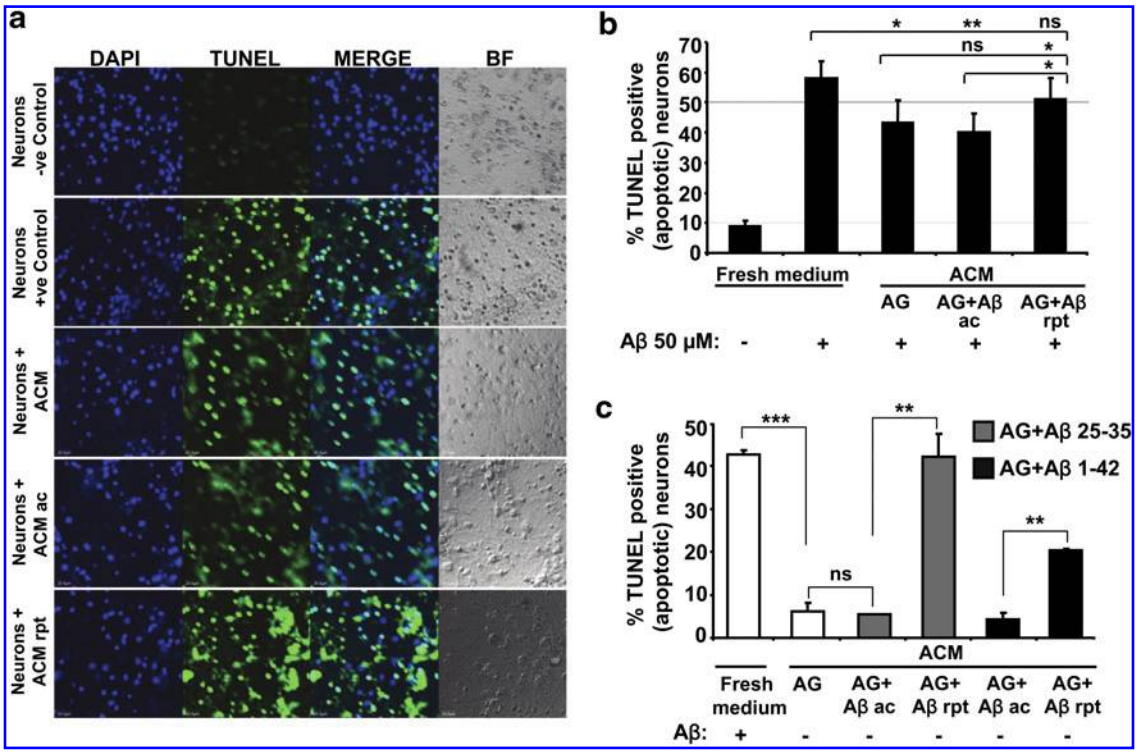

FIG. 9. Repeated Aβ treatment abrogates the neuroprotective effect of astrocytes. Primary murine cortical neurons were treated **(a, b)** or untreated **(c)** with Aβ (50 μM) for ~14 h in the presence of either fresh or conditioned medium from astrocytes that were either untreated or treated with either 25–35 (a, b) or 1–42 (c) Aβ (acute or repeated) for 12–14 h. Bar graphs represent the mean ± SD of apoptotic neuronal cells measured by TUNEL labeling as a percentage of total cells (labeled by Hoechst). **(a)** Representative micrographs of apoptotic neurons are presented. **(b,c)** Quantitative analysis of microscopic data from 2 independent experiments. For statistical analysis, at least 1000–2000 cells were counted from each experiment and are shown as mean ± SD. $^{*}p \leq 0.05$, $^{**}p \leq 0.01$, $^{***}p \leq 0.001$, ns, not significant.

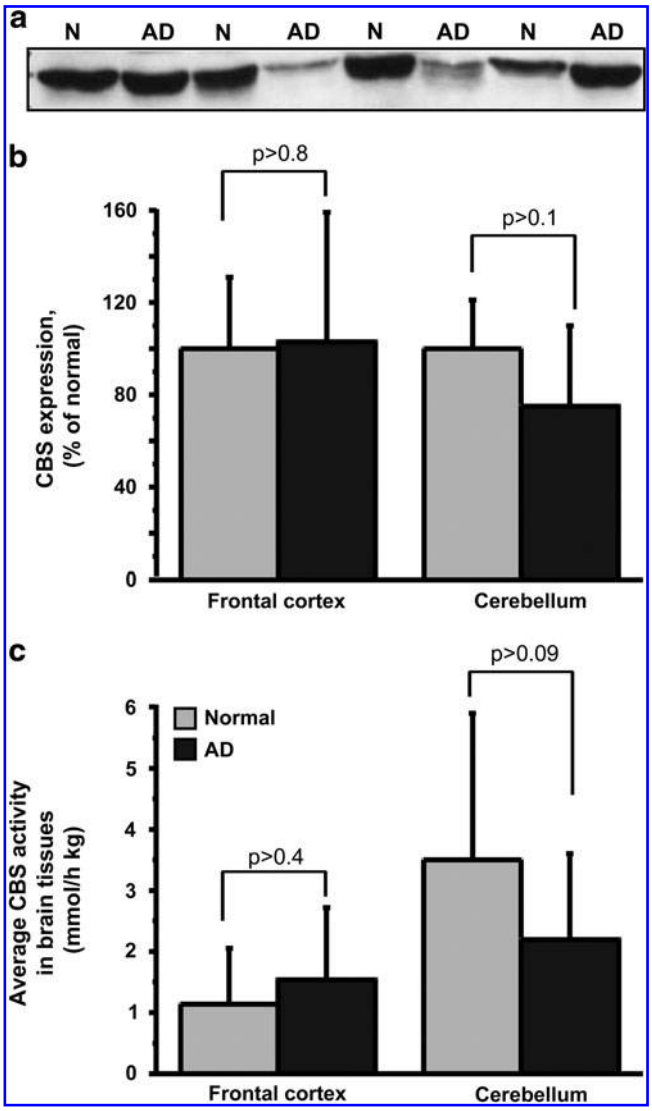

FIG. 10. CBS activity and protein expression levels are diminished in cerebellum of AD patients. (a) Representative Western blot analysis showing CBS levels in postmortem cerebellum of AD patients and age-matched normal individuals. N and AD denote normal and AD samples, respectively. **(b)** The average CBS protein levels ($n=8$), and **(c)** the average CBS activity in postmortem samples of frontal cortex ($n=10$) and cerebellum ($n=12$ and 16 for normal and AD samples respectively), obtained from AD patients and age-matched normal individuals. The CBS protein levels were quantified from Western blots. AD, Alzheimer's disease.

significant thiol-based redox buffer outside the cell (33). A reductive shift (*i.e.*, to a more negative redox potential value) is associated with cellular proliferation, whereas an oxidative shift correlates with cell death (33). Our results, that is, that Aβ treatment induces a reductive shift, in contrast to a general oxidant, in the extracellular redox potential in astrocytic cultures, suggest that a similar response in the CNS might stimulate proliferation of microglia, exacerbating neuronal degeneration. In fact, inflammation is considered to contribute to neuronal demise in AD (4).

Our study also reveals that the astrocytic redox response to Aβ stimulation is complex and distinct in the intra- *versus* extracellular compartments. Paradoxically, elevated H_2O_2 levels are observed under conditions where there is a net shift in the extracellular redox potential in the reductive direction in response to Aβ treatment (Figs. 3–5), emphasizing the importance of analyzing metabolic responses to oxidative stress in the context of the redox milieu in addition to the levels of the individual oxidant species. Ectodomains of membrane proteins are rich in disulfide bonds, and the $\sim$30 mV decrease in redox potential induced by repeated Aβ treatment (Figs. 4 and 5) is expected to result in a 10-fold shift in the equilibrium from the disulfide to the dithiol state. The redox state of receptors and transporters influence both their structure and function and the Aβ-induced reductive shift is likely to have pleiotropic consequences on signaling pathways emanating from redox-sensitive membrane protein targets that await elucidation.

An interesting parallel in extracellular reductive remodeling is seen with dendritic cells during activation of T cells and results from increased cystine consumption and extracellular cysteine secretion without enhanced transsulfuration flux (49). The released cysteine is used by naïve T cells, which, like neurons, are unable to efficiently transport cystine. In the CNS, cysteine accumulation, if unchecked, might lead to N-methyl D-aspartate receptor excitoxicity (36). We speculate that the threshold between a neuroprotective *versus* toxic concentration of cysteine may be crossed if astrocytes are overactivated by repeated Aβ stimulation. As previously shown with dendritic cells, the γ-glutamyl cycle is also the source of extracellular GSH and cysteine in astrocytes (49). Inhibition of the x_C^- antiporter, the GSH exporter or γ-glutamyltranspeptidase all lead to lower extracellular cysteine accumulation (Fig. 7a). While secretion of extracellular thioredoxin by dendritic cells during T cell activation was proposed to contribute to cysteine accumulation (7), subsequent studies have ruled out a role for thioredoxin in this process (49). Additional redox systems not examined in this study are also likely to contribute to the redox remodeling induced by Aβ, For instance, a Cu-Zn-type extracellular SOD has been shown to delay oxidation of extracellular GSH (45).

The profiles of intracellular redox responses elicited by acute *versus* repeated exposure to Aβ are also distinct from the corresponding response triggered by t-BuOOH (Fig. 1b). Astrocytes responded to peroxide treatment by a compensatory increase in GSH synthesis, without affecting CBS enzyme level, leading to a net reductive shift in the intracellular GSH/GSSG potential (Fig. 3). Although t-BuOOH treatment does not affect CBS levels, flux through the transsulfuration flux is increased and could result from changes either up- or downstream of CBS, which remain to be elucidated. The GSH:GSSG ratio is initially diminished in response to acute ($\sim$30%) and chronic ($\sim$50%) t-BuOOH treatment at 6 h but subsequently overshoots the control values at 12 h (Fig. 3h). In an autocorrective response, cells increase GSH synthesis to counter oxidative stress, leading to more reducing redox potential at 12 h. Cells treated repeatedly with t-BuOOH show a different response, that is, lower GSSG levels (Fig. 3e). The net result, nevertheless, is more reducing conditions.

In contrast, both acute and repeated Aβ treatment resulted in an oxidative shift in the GSH/GSSG redox potential. With acute Aβ treatment, the decline in the redox potential was driven by the time-dependent increase in GSSG levels, whereas with repeated Aβ treatment, the concentration of GSSG increased transiently before returning to control levels (Fig. 3e). However, the concentration of reduced GSH also

decreased over time with chronic Aβ treatment, which resulted in a lower redox potential. The difference between the acute *versus* repeated response to Aβ suggests that metabolic adaptation occurs during prolonged Aβ treatment that results in lowering of the GSSG pool. Since the astrocytic GSH pool also serves as an important cysteine reservoir for supporting neuronal GSH synthesis *via* secretion and cleavage, the smaller GSH pool size due to extended Aβ exposure could compromise this neuroprotective function of astrocytes.

CBS protein levels were diminished after repeated Aβ but not peroxide treatment (Fig. 3g). A similar trend was observed in cerebellar CBS levels and activity in AD *versus* control samples, but did not reach statistical significance (Fig. 10). This could have resulted from large inter-individual variations, the relatively small sample size as well as sample heterogeneity, that is, if decreased CBS were restricted to astrocytes in AD, the difference would be underestimated in tissue samples due to the presence of nonastrocytic cells. Since CBS plays an important role both in GSH-linked redox homeostasis (10, 35) and in H_2S biogenesis (44), reduced expression of this protein in AD brain if seen might be significant in disease pathology. H_2S, which modifies long-term potentiation (1), is reported to be severely depressed in AD brain (17). In addition, levels of S-adenosylmethionine, an allosteric activator (18) and stabilizer (39) of CBS, are decreased in AD brain, but not in idiopathic Parkinson's disease patients, suggesting that the change is not generally correlated with a chronic neurodegenerative disease but may be AD specific (34). Hence, upregulation of CBS expression or its activation or stabilization might represent a specific therapeutic strategy for alleviating redox perturbations associated with AD.

NAC treatment or catalase overexpression abrogated the Aβ-induced ROS generation (Fig. 2). Catalase or SOD overexpression have been shown to decrease ROS levels and rescue neurons from the toxic action of the Aβ peptide (16, 30), consistent with overproduction of ROS contributing to neurotoxicity. Our finding that catalase but not SOD1 levels were diminished after repeated Aβ treatment is consistent with the earlier observation that brain catalase but not SOD activity is decreased in patients with Alzheimer's type dementia (23, 40). Ferritin and catalase are potent suppressors of Aβ toxicity (41). For to be effective against Aβ-induced ROS accumulation, downstream antioxidant enzymes such as catalase and/or GSH peroxidase, which remove H_2O_2, the product of SOD, need to be also act in concert. A direct effect of Aβ on catalase has been shown, which resulted in deactivation of catalase and increased cellular intracellular H_2O_2 (25). Although some studies report decreased SOD activity (31, 48), others report either no change (23, 40) or increased SOD activity in AD patients compared with controls (28).

Clearly, the Aβ effects on redox homeostasis are more complex than simply being mediated *via* peroxide as proposed (11). The aim of the present study was to determine differences, if any in astrocytic responses to a specific (*e.g.*, Aβ) *versus* a general (*e.g.*, t-BuOOH) oxidant insult. In the present study, we report for the first time, a detailed mechanistic analysis of the redox changes in astrocytes in response to Aβ treatment. Although Aβ treatment stimulates H_2O_2/ROS production in astrocytes, the intra- and extra-cellular metabolic responses are distinct from those of a nonspecific oxidant, and await full mechanistic elucidation. In summary, our study points to the importance of identifying AD-specific redox markers that might be etiologically important and could serve as potential therapeutic targets.

Acknowledgments

This work was supported in part by grants from the National Institutes of Health (DK64959). Support for the Michigan Alzheimer's Disease Research Center (5P50 AG008761) from the National Institutes of Health is gratefully acknowledged. This work utilized the Morphology and Image Analysis Cores of the Michigan Diabetes Research and Training Center funded by NIH5P60 DK20572 from the National Institute of Diabetes & Digestive & Kidney Diseases.

Author Disclosure Statement

No competing financial interests exist.

References

1. Abe K and Kimura H. The possible role of hydrogen sulfide as an endogenous neuromodulator. *J Neurosci* 16: 1066–1071, 1996.
2. Abramov AY, Canevari L, and Duchen MR. Changes in intracellular calcium and glutathione in astrocytes as the primary mechanism of amyloid neurotoxicity. *J Neurosci* 23: 5088–5095, 2003.
3. Abramov AY, Canevari L, and Duchen MR. Beta-amyloid peptides induce mitochondrial dysfunction and oxidative stress in astrocytes and death of neurons through activation of NADPH oxidase. *J Neurosci* 24: 565–575, 2004.
4. Akiyama H, Barger S, Barnum S, Bradt B, Bauer J, Cole GM, Cooper NR, Eikelenboom P, Emmerling M, Fiebich BL, Finch CE, Frautschy S, Griffin WS, Hampel H, Hull M, Landreth G, Lue L, Mrak R, Mackenzie IR, McGeer PL, O'Banion MK, Pachter J, Pasinetti G, Plata-Salaman C, Rogers J, Rydel R, Shen Y, Streit W, Strohmeyer R, Tooyoma I, Van Muiswinkel FL, Veerhuis R, Walker D, Webster S, Wegrzyniak B, Wenk G, and Wyss-Coray T. Inflammation and Alzheimer's disease. *Neurobiol Aging* 21: 383–421, 2000.
5. Allaman I, Gavillet M, Belanger M, Laroche T, Viertl D, Lashuel HA, and Magistretti PJ. Amyloid-beta aggregates cause alterations of astrocytic metabolic phenotype: impact on neuronal viability. *J Neurosci* 30: 3326–3338, 2010.
6. Andersen JK. Oxidative stress in neurodegeneration: cause or consequence? *Nat Med* 10 Suppl: S18–S25, 2004.
7. Angelini G, Gardella S, Ardy M, Ciriolo MR, Filomeni G, Di Trapani G, Clarke F, Sitia R, and Rubartelli A. Antigen-presenting dendritic cells provide the reducing extracellular microenvironment required for T lymphocyte activation. *Proc Natl Acad Sci USA* 99: 1491–1496, 2002.
8. Banerjee R, Vitvitsky V, and Garg SK. The undertow of sulfur metabolism on glutamatergic neurotransmission. *Trends Biochem Sci* 33: 413–419, 2008.
9. Banerjee R and Zou CG. Redox regulation and reaction mechanism of human cystathionine-beta-synthase: a PLP-dependent hemesensor protein. *Arch Biochem Biophys* 433: 144–156, 2005.
10. Beatty PW and Reed DJ. Involvement of the cystathionine pathway in the biosynthesis of glutathione by isolated rat hepatocytes. *Arch Biochem Biophys* 204: 80–87, 1980.
11. Behl C, Davis JB, Lesley R, and Schubert D. Hydrogen peroxide mediates amyloid beta protein toxicity. *Cell* 77: 817–827, 1994.

12. Butterfield DA, Drake J, Pocernich C, and Castegna A. Evidence of oxidative damage in Alzheimer's disease brain: central role for amyloid beta-peptide. *Trends Mol Med* 7: 548–554, 2001.
13. Consensus recommendations for the postmortem diagnosis of Alzheimer's disease. The National Institute on Aging, and Reagan Institute Working Group on Diagnostic Criteria for the Neuropathological Assessment of Alzheimer's Disease. *Neurobiol Aging* 18: S1–S2, 1997.
14. Dringen R, Gutterer JM, and Hirrlinger J. Glutathione metabolism in brain metabolic interaction between astrocytes and neurons in the defense against reactive oxygen species. *Eur J Biochem* 267: 4912–4916, 2000.
15. Dringen R, Pfeiffer B, and Hamprecht B. Synthesis of the antioxidant glutathione in neurons: supply by astrocytes of CysGly as precursor for neuronal glutathione. *J Neurosci* 19: 562–569, 1999.
16. Dumont M, Wille E, Stack C, Calingasan NY, Beal MF, and Lin MT. Reduction of oxidative stress, amyloid deposition, and memory deficit by manganese superoxide dismutase overexpression in a transgenic mouse model of Alzheimer's disease. *FASEB J* 23: 2459–2466, 2009.
17. Eto K, Asada T, Arima K, Makifuchi T, and Kimura H. Brain hydrogen sulfide is severely decreased in Alzheimer's disease. *Biochem Biophys Res Commun* 293: 1485–1488, 2002.
18. Finkelstein JD, Kyle WE, Martin JL, and Pick AM. Activation of cystathionine synthase by adenosylmethionine and adenosylethionine. *Biochem Biophys Res Commun* 66: 81–87, 1975.
19. Garg S, Vitvitsky V, Gendelman HE, and Banerjee R. Monocyte differentiation, activation, and mycobacterial killing are linked to transsulfuration-dependent redox metabolism. *J Biol Chem* 281: 38712–38720, 2006.
20. Garg SK, Banerjee R, and Kipnis J. Neuroprotective immunity: T cell-derived glutamate endows astrocytes with a neuroprotective phenotype. *J Immunol* 180: 3866–3873, 2008.
21. Garg SK, Kipnis J, and Banerjee R. IFN-gamma and IL-4 differentially shape metabolic responses and neuroprotective phenotype of astrocytes*. *J Neurochem* 108: 1155–1166, 2009.
22. Go YM and Jones DP. Redox compartmentalization in eukaryotic cells. *Biochim Biophys Acta* 1780: 1273–1290, 2008.
23. Gsell W, Conrad R, Hickethier M, Sofic E, Frolich L, Wichart I, Jellinger K, Moll G, Ransmayr G, Beckmann H, *et al.* Decreased catalase activity but unchanged superoxide dismutase activity in brains of patients with dementia of Alzheimer type. *J Neurochem* 64: 1216–1223, 1995.
24. Gunasingh MJ, Philip JE, Ashok BS, Kirubagaran R, Jebaraj WC, Davis GD, Vignesh S, Dhandayuthapani S, and Jayakumar R. Melatonin prevents amyloid protofibrillar induced oxidative imbalance and biogenic amine catabolism. *Life Sci* 83: 96–102, 2008.
25. Habib LK, Lee MT, and Yang J. Inhibitors of catalase-amyloid interactions protect cells from beta-amyloid-induced oxidative stress and toxicity. *J Biol Chem* 285: 38933–38943, 2010.
26. Hattori N, Kitagawa K, Higashida T, Yagyu K, Shimohama S, Wataya T, Perry G, Smith MA, and Inagaki C. CI-ATPase and Na+/K(+)-ATPase activities in Alzheimer's disease brains. *Neurosci Lett* 254: 141–144, 1998.
27. Hernandez-Guillamon M, Delgado P, Ortega L, Pares M, Rosell A, Garcia-Bonilla L, Fernandez-Cadenas I, Borrell-Pages M, Boada M, and Montaner J. Neuronal TIMP-1 release accompanies astrocytic MMP-9 secretion and enhances astrocyte proliferation induced by beta-amyloid 25–35 fragment. *J Neurosci Res* 87: 2115–2125, 2009.
28. Kharrazi H, Vaisi-Raygani A, Rahimi Z, Tavilani H, Aminian M, and Pourmotabbed T. Association between enzymatic and non-enzymatic antioxidant defense mechanism with apolipoprotein E genotypes in Alzheimer disease. *Clin Biochem* 41: 932–936, 2008.
29. Lauderback CM, Hackett JM, Huang FF, Keller JN, Szweda LI, Markesbery WR, and Butterfield DA. The glial glutamate transporter, GLT-1, is oxidatively modified by 4-hydroxy-2-nonenal in the Alzheimer's disease brain: the role of Abeta1-42. *J Neurochem* 78: 413–416, 2001.
30. Manelli AM and Puttfarcken PS. beta-Amyloid-induced toxicity in rat hippocampal cells: *in vitro* evidence for the involvement of free radicals. *Brain Res Bull* 38: 569–576, 1995.
31. Marcus DL, Thomas C, Rodriguez C, Simberkoff K, Tsai JS, Strafaci JA, and Freedman ML. Increased peroxidation and reduced antioxidant enzyme activity in Alzheimer's disease. *Exp Neurol* 150: 40–44, 1998.
32. Mattson MP. Pathways towards and away from Alzheimer's disease. *Nature* 430: 631–639, 2004.
33. Moriarty-Craige SE and Jones DP. Extracellular thiols and thiol/disulfide redox in metabolism. *Annu Rev Nutr* 24: 481–509, 2004.
34. Morrison LD, Smith DD, and Kish SJ. Brain S-adenosylmethionine levels are severely decreased in Alzheimer's disease. *J Neurochem* 67: 1328–1331, 1996.
35. Mosharov E, Cranford MR, and Banerjee R. The quantitatively important relationship between homocysteine metabolism and glutathione synthesis by the transsulfuration pathway and its regulation by redox changes. *Biochemistry* 39: 13005–13011, 2000.
36. Olney JW, Zorumski C, Price MT, and Labruyere J. L-cysteine, a bicarbonate-sensitive endogenous excitotoxin. *Science* 248: 596–599, 1990.
37. Pike CJ, Burdick D, Walencewicz AJ, Glabe CG, and Cotman CW. Neurodegeneration induced by beta-amyloid peptides *in vitro*: the role of peptide assembly state. *J Neurosci* 13: 1676–1687, 1993.
38. Pike CJ, Cummings BJ, Monzavi R, and Cotman CW. Beta-amyloid-induced changes in cultured astrocytes parallel reactive astrocytosis associated with senile plaques in Alzheimer's disease. *Neuroscience* 63: 517–531, 1994.
39. Prudova A, Bauman Z, Braun A, Vitvitsky V, Lu SC, and Banerjee R. S-adenosylmethionine stabilizes cystathionine beta-synthase and modulates redox capacity. *Proc Natl Acad Sci USA* 103: 6489–6494, 2006.
40. Ramassamy C, Averill D, Beffert U, Bastianetto S, Theroux L, Lussier-Cacan S, Cohn JS, Christen Y, Davignon J, Quirion R, and Poirier J. Oxidative damage and protection by antioxidants in the frontal cortex of Alzheimer's disease is related to the apolipoprotein E genotype. *Free Radic Biol Med* 27: 544–553, 1999.
41. Rival T, Page RM, Chandraratna DS, Sendall TJ, Ryder E, Liu B, Lewis H, Rosahl T, Hider R, Camargo LM, Shearman MS, Crowther DC, and Lomas DA. Fenton chemistry and oxidative stress mediate the toxicity of the beta-amyloid peptide in a Drosophila model of Alzheimer's disease. *Eur J Neurosci* 29: 1335–1347, 2009.
42. Robert K, Vialard F, Thiery E, Toyama K, Sinet PM, Janel N, and London J. Expression of the cystathionine beta synthase (CBS) gene during mouse development and immunolocalization in adult brain. *J Histochem Cytochem* 51: 363–371, 2003.
43. Schafer FQ and Buettner GR. Redox environment of the cell as viewed through the redox state of the glutathione disulfide/glutathione couple. *Free Radic Biol Med* 30: 1191–1212, 2001.
44. Singh S, Madzelan P, Stasser J, Weeks CL, Becker D, Spiro TG, Penner-Hahn J, and Banerjee R. Modulation of the heme

electronic structure and cystathionine beta-synthase activity by second coordination sphere ligands: the role of heme ligand switching in redox regulation. *J Inorg Biochem* 103: 689–697, 2009.
45. Stewart VC, Stone R, Gegg ME, Sharpe MA, Hurst RD, Clark JB, and Heales SJ. Preservation of extracellular glutathione by an astrocyte derived factor with properties comparable to extracellular superoxide dismutase. *J Neurochem* 83: 984–991, 2002.
46. Vitvitsky V, Dayal S, Stabler S, Zhou Y, Wang H, Lentz SR, and Banerjee R. Perturbations in homocysteine-linked redox homeostasis in a murine model for hyperhomocysteinemia. *Am J Physiol Regul Integr Comp Physiol* 287: R39–R46, 2004.
47. Vitvitsky V, Thomas M, Ghorpade A, Gendelman HE, and Banerjee R. A functional transsulfuration pathway in the brain links to glutathione homeostasis. *J Biol Chem* 281: 35785–35793, 2006.
48. Vural H, Demirin H, Kara Y, Eren I, and Delibas N. Alterations of plasma magnesium, copper, zinc, iron and selenium concentrations and some related erythrocyte antioxidant enzyme activities in patients with Alzheimer's disease. *J Trace Elem Med Biol* 24: 169–173, 2010.
49. Yan Z, Garg SK, Kipnis J, and Banerjee R. Extracellular redox modulation by regulatory T cells. *Nat Chem Biol* 5: 721–723, 2009.

Address correspondence to:
Prof. Ruma Banerjee
Department of Biochemistry
University of Michigan Medical School
Ann Arbor, MI 48109-0600

E-mail: rbanerje@umich.edu

Date of first submission to ARS Central, October 3, 2010; date of final revised submission, January 11, 2011; date of acceptance, January 14, 2011.

Abbreviations Used

Aβ = amyloid beta
AβH = aspartate-β-hydroxamate
ac = acute
ACV = acivicin
AD = Alzheimer's disease
Aza = azaserine
CBS = cystathionine β-synthase
Cys = cysteine
Cys_2 = cystine
GSSG = glutathione disulfide
GSH = glutathione
MRP1 = multidrug resistance protein 1
MTT = (3-(4,5-dimethylthiazol-2yl)-2,5-diphenyltetrazolium bromide)
NAC = N-acetyl cysteine
PPG = propargylglycine
ROS = reactive oxygen species
rpt = repeated
SAS = sulfasalazine
SOD = superoxide dismutase
t-BuOOH = tertiary-butylhydroperoxide
TUNEL = terminal deoxynucleotidyl transferase-dUTP nick end labeling

This article has been cited by:

1. Shannon Rose, Stepan Melnyk, Timothy A. Trusty, Oleksandra Pavliv, Lisa Seidel, Jingyun Li, Todd Nick, S. Jill James. 2012. Intracellular and Extracellular Redox Status and Free Radical Generation in Primary Immune Cells from Children with Autism. *Autism Research and Treatment* **2012**, 1-10. [CrossRef]